J|A|C|S ARTICLES

Published on Web 12/29/2008

Synthesis, Photophysical Behavior, and Electronic Structure of Push−Pull Purines

Roslyn S. Butler, Pamela Cohn, Phillip Tenzel, Khalil A. Abboud, and Ronald K. Castellano*

Department of Chemistry, University of Florida, P.O. Box 117200, Gainesville, Florida 32611-7200

Received August 18, 2008; E-mail: castellano@chem.ufl.edu

Abstract: "Push−pull" purines have been synthesized by the introduction of electron-accepting functional groups (**A** = CN, CO_2Me, and CONHR) to the heterocyclic C(8) position to complement typical electron-donating substituents at C(2) (**D**[1]) and C(6) (**D**[2]). The donor−acceptor purines show significantly altered, and overall improved photophysical properties relative to their acceptor-free precursors (**A** = H); these include red-shifted (20−50 nm) absorption maxima, highly solvatochromic emission profiles (em λ_{max} from 355−466 nm depending on substitution pattern and solvent) with excellent linear correlations between emission energy and solvent polarity (E_T^N), improved photochemical stability upon continuous irradiation, and enhanced (up to 2500%) fluorescence quantum yields. Comprehensive structure−property studies show how the absorption/emission maxima and quantum yields depend on donor and acceptor structure, relative donor position (C(2) or C(6)), and solvent (1,4-dioxane, dichloromethane, acetonitrile, methanol, and in some cases water). Further insight regarding electronic structure comes from a quantitative treatment of the solvent-dependent emission data (that provides $\Delta\mu_{ge}$ values ranging from 1.9 to 3.4 D) and DFT (B3LYP/6-311++G**) electronic structure calculations. X-ray crystal structures of several derivatives showcase the molecular recognition capabilities of the donor−acceptor chromophores that overall have photophysical and structural properties suitable for applications in biosensing and materials.

Introduction

Simple nucleobase heterocycles are attractive as "functional" π components in organic materials[1] wherein their built-in molecular recognition features can be brought to bear on solution-phase, solid-state, and surface architectures,[2,3] and even bulk transport or magnetic properties and device performance.[4,5] Unlike other heterocycles,[6] some with biological relevance (e.g., porphyrins[7]), the nucleobases have sparsely been considered for materials applications that rely on their photophysical properties.[8] This is in part due to the exceedingly low fluorescence quantum yields (Φ_F) of the purines and pyrimidines; values on the order of 0.01% in water are typical.[9] Remarkable improvements to the intrinsic fluorescence properties of nucleobases have, however, been achieved for biological applications,[10] where designer molecules routinely play a role in sensing and reporting.[11,12] Some recent examples that are particularly

(1) For relevant reviews see:(a) Sessler, J. L.; Lawrence, C. M.; Jayawickramarajah, J. *Chem. Soc. Rev.* **2007**, *36*, 314–325. (b) Davis, J. T.; Spada, G. P. *Chem. Soc. Rev.* **2007**, *36*, 296–313. (c) Weck, M. *Polym. Int.* **2007**, *56*, 453–460. (d) Hoeben, F. J. M.; Jonkheijm, P.; Meijer, E. W.; Schenning, A. *Chem. Rev.* **2005**, *105*, 1491–1546. (e) Sivakova, S.; Rowan, S. J. *Chem. Soc. Rev.* **2005**, *34*, 9–21. (f) Araki, K.; Yoshikawa, I. *Top. Curr. Chem.* **2005**, *256*, 133–165.

(2) Representative recent examples:(a) Numata, M.; Sugiyasu, K.; Kishida, T.; Haraguchi, S.; Fujita, N.; Park, S. M.; Yun, Y. J.; Kim, B. H.; Shinkai, S. *Org. Biomol. Chem* **2008**, *6*, 712–718. (b) Jatsch, A.; Kopyshev, A.; Mena-Osteritz, E.; Bäuerle, P. *Org. Lett.* **2008**, *10*, 961–964. (c) Yoshikawa, I.; Sawayama, J.; Araki, K. *Angew. Chem., Int. Ed.* **2008**, *47*, 1038–1041. (d) Spada, G. P.; Lena, S.; Masiero, S.; Pieraccini, S.; Surin, M.; Samorì, P. *Adv. Mater.* **2008**, *20*, 2433–2438. (e) Mather, B. D.; Baker, M. B.; Beyer, F. L.; Berg, M. A. G.; Green, M. D.; Long, T. E. *Macromolecules* **2007**, *40*, 6834–6845. (f) Arnal-Hérault, C.; Barboiu, M.; Pasc, A.; Michau, M.; Perriat, P.; van der Lee, A. *Chem. Eur. J.* **2007**, *13*, 6792–6800. (g) Sreenivasachary, N.; Hickman, D. T.; Sarazin, D.; Lehn, J.-M. *Chem. Eur. J.* **2006**, *12*, 8581–8588. (h) Spijker, H. J.; Dirks, A. J.; van Hest, J. C. M. *J. Polym. Sci., Part A: Polym. Chem.* **2006**, *44*, 4242–4250. (i) Park, T.; Zimmerman, S. C.; Nakashima, S. *J. Am. Chem. Soc.* **2005**, *127*, 6520–6521. (j) Norsten, T. B.; Jeoung, E.; Thibault, R. J.; Rotello, V. M. *Langmuir* **2003**, *19*, 7089–7093.

(3) (a) Kumar, A. M. S.; Sivakova, S.; Marchant, R. E.; Rowan, S. J. *Small* **2007**, *3*, 783–787. (b) Sivakova, S.; Wu, J.; Campo, C. J.; Mather, P. T.; Rowan, S. J. *Chem. Eur. J.* **2006**, *12*, 446–456. (c) Sivakova, S.; Bohnsack, D. A.; Mackay, M. E.; Suwanmala, P.; Rowan, S. J. *J. Am. Chem. Soc.* **2005**, *127*, 18202–18211.

(4) (a) Lena, S.; Brancolini, G.; Gottarelli, G.; Mariani, P.; Masiero, S.; Venturini, A.; Palermo, V.; Pandoli, O.; Pieraccini, S.; Samorì, P.; Spada, G. P. *Chem. Eur. J.* **2007**, *13*, 3757–3764. (b) Maruccio, G.; Visconti, P.; Arima, V.; D'Amico, S.; Blasco, A.; D'Amone, E.; Cingolani, R.; Rinaldi, R.; Masiero, S.; Giorgi, T.; Gottarelli, G. *Nano Lett.* **2003**, *3*, 479–483. (c) D'Amico, S.; Maruccio, G.; Visconti, P.; D'Amone, E.; Cingolani, R.; Rinaldi, R.; Masiero, S.; Spada, G. P.; Gottarelli, G. *Microelectron. J.* **2003**, *34*, 961–963. (d) Rinaldi, R.; Maruccio, G.; Biasco, A.; Arima, V.; Cingolani, R.; Giorgi, T.; Masiero, S.; Spada, G. P.; Gottarelli, G. *Nanotechnology* **2002**, *13*, 398–403. (e) Rinaldi, R.; Branca, E.; Cingolani, R.; Masiero, S.; Spada, G. P.; Gottarelli, G. *Appl. Phys. Lett.* **2001**, *78*, 3541–3543.

(5) (a) Murata, T.; Saito, G.; Enomoto, Y.; Honda, G.; Shimizu, Y.; Matsui, S.; Sakata, M.; Drozdova, O. O.; Yakushi, K. *Bull. Chem. Soc. Jpn.* **2008**, *81*, 331–344. (b) Tanaka, H.; Shiomi, D.; Ise, T.; Sato, K.; Takui, T. *CrystEngComm* **2007**, *9*, 767–771.

(6) Forrest, S. R.; Thompson, M. E. *Chem. Rev.* **2007**, *107*, 923–925.

(7) See, for example: Barker, C. A.; Zeng, X.; Bettington, S.; Batsanov, A. S.; Bryce, M. R.; Beeby, A. *Chem. Eur. J.* **2007**, *13*, 6710–6717.

(8) Kim, S. J.; Kool, E. T. *J. Am. Chem. Soc.* **2006**, *128*, 6164–6171.

(9) (a) Andréasson, J.; Holmén, A.; Albinsson, B. *J. Phys. Chem. B* **1999**, *103*, 9782–9789. (b) Wilson, R. W.; Callis, P. R. *Photochem. Photobiol.* **1980**, *31*, 323–327. (c) Ward, D. C.; Reich, E.; Stryer, L. *J. Biol. Chem.* **1969**, *244*, 1228–1237. (d) Drobnik, J.; Augenstein, L. *Photochem. Photobiol.* **1966**, *5*, 13–30.

relevant to the current work show how extension of the nucleobase conjugated system by even a vinyl group[12i] or aromatic ring[11e,f,12d] is sufficient to produce highly emissive species that are also capable of base pairing.

2-Aminopurine (2-AP), an isomer of adenine, remains perhaps the simplest functional nucleobase variant that is also fluorescent; a high quantum yield (68% in water for the riboside)[9c] underlies its widespread usage as an optical probe[13] and continued mechanistic and structural study.[14] Even so, molecules based on this platform have sparsely filtered into traditional organic materials and related sensing applications,[8,15] and in surprisingly few cases has their optimization and broader photophysical evaluation (e.g., studies in nonaqueous solution or the bulk) toward this goal been performed.

Shown here is how the donor-π-acceptor design, commonly used to tailor the optical and electronic properties of π-conjugated systems,[16−19] can be usefully extended to 2-AP and related purines (Figure 1).[20] Significant photophysical changes occur upon introduction of acceptor substituents to the purine C(8) position that complement typical donor groups at C(2) and C(6). The arrangement affords increased quantum yields (in many cases near unity) and significantly red-shifted absorption/emission spectra in organic solution (and even water) relative to the acceptor-free molecules; methyl ester functionalization of 2-amino-9-benzylpurine, for example, imparts a 13-fold quantum yield increase in 1,4-dioxane (other derivatives show up to 25-fold increases). Photophysical studies in multiple solvents, X-ray crystallography, and theoretical analysis show how the nature (and position) of the donor and acceptor groups contribute to the optical parameters, solid-state ordering, and electronic structure of the purines.

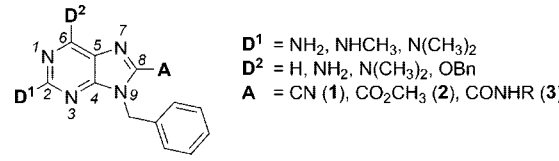

Figure 1. Generic structure of the donor−acceptor purines considered in this work (D = donor; A = acceptor; Bn = benzyl). Important atoms have been numbered in the conventional way around the purine core.

The current investigation includes synthesis of among the first carboxamide derivatives **3** (Figure 1), that despite bearing a

(10) For recent reviews see:(a) Venkatesan, N.; Seo, Y. J.; Kim, B. H. *Chem. Soc. Rev.* **2008**, *37*, 648–663. (b) Tor, Y. *Tetrahedron* **2007**, *63*, 3425–3426. (c) Asseline, U. *Curr. Org. Chem.* **2006**, *10*, 491–518. (d) Wilson, J. N.; Kool, E. T. *Org. Biomol. Chem.* **2006**, *4*, 4265–4274. (e) Rist, M. J.; Marino, J. P. *Curr. Org. Chem.* **2002**, *6*, 775–793.

(11) (a) Srivatsan, S. G.; Weizman, H.; Tor, Y. *Org. Biomol. Chem.* **2008**, *6*, 1334–1338. (b) Tor, Y.; Del Valle, S.; Jaramillo, D.; Srivatsan, S. G.; Rios, A.; Weizman, H. *Tetrahedron* **2007**, *63*, 3608–3614. (c) Srivatsan, S. G.; Tor, Y. *Tetrahedron* **2007**, *63*, 3601–3607. (d) Srivatsan, S. G.; Tor, Y. *J. Am. Chem. Soc.* **2007**, *129*, 2044–2053. (e) Greco, N. J.; Tor, Y. *Tetrahedron* **2007**, *63*, 3515–3527. (f) Greco, N. J.; Tor, Y. *J. Am. Chem. Soc.* **2005**, *127*, 10784–10785.

(12) For additional recent examples:(a) Wilson, J. N.; Cho, Y.; Tan, S.; Cuppoletti, A.; Kool, E. T. *ChemBioChem* **2008**, *9*, 279–285. (b) Seela, F.; Sirivolu, V. R. *Org. Biomol. Chem.* **2008**, *6*, 1674–1687. (c) Sandin, P.; Börjesson, K.; Li, H.; Mårtensson, J.; Brown, T.; Wilhelmsson, L. M.; Albinsson, B. *Nucleic Acids Res.* **2008**, *36*, 157–167. (d) Mitsui, T.; Kimoto, M.; Kawai, R.; Yokoyama, S.; Hirao, I. *Tetrahedron* **2007**, *63*, 3528–3537. (e) Mizuta, M.; Seio, K.; Miyata, K.; Sekine, M. *J. Org. Chem.* **2007**, *72*, 5046–5055. (f) Firth, A. G.; Fairlamb, I. J. S.; Darley, K.; Baumann, C. G. *Tetrahedron Lett.* **2006**, *47*, 3529–3533. (g) Martí, A. A.; Jockusch, S.; Li, Z.; Ju, J.; Turro, N. J. *Nucleic Acids Res.* **2006**, *34*, e50. (h) Sharon, E.; Lévesque, S. A.; Munkonda, M. N.; Sévigny, J.; Ecke, D.; Reiser, G.; Fischer, B. *ChemBioChem* **2006**, *7*, 1361–1374. (i) Gaied, N. B.; Glasser, N.; Ramalanjaona, N.; Beltz, H.; Wolff, P.; Marquet, R.; Burger, A.; Mély, Y. *Nucleic Acids Res.* **2005**, *33*, 1031–1039. (j) Okamoto, A.; Saito, Y.; Saito, I. *J. Photochem. Photobiol. C* **2005**, *6*, 108–122.

(13) See, for example: Ballin, J. D.; Bharill, S.; Fialcowitz-White, E. J.; Gryczynski, I.; Gryczynski, Z.; Wilson, G. M. *Biochemistry* **2007**, *46*, 13948–13960.

(14) (a) Kodali, G.; Kistler, K. A.; Matsika, S.; Stanley, R. J. *J. Phys. Chem. B* **2008**, *112*, 1789–1795. (b) Bharill, S.; Sarkar, P.; Ballin, J. D.; Gryczynski, I.; Wilson, G. M.; Gryczynski, Z. *Anal. Biochem.* **2008**, *377*, 141–149. (c) Neely, R. K.; Magennis, S. W.; Parsons, S.; Jones, A. C. *ChemPhysChem* **2007**, *8*, 1095–1102. (d) Serrano-Andrés, L.; Merchán, M.; Borin, A. C. *Proc. Natl. Acad. Sci. U.S.A.* **2006**, *103*, 8691–8696. (e) He, R.-X.; Duan, X.-H.; Li, X.-Y. *Phys. Chem. Chem. Phys.* **2006**, *8*, 587–591. (f) Perun, S.; Sobolewski, A. L.; Domcke, W. *Mol. Phys.* **2006**, *104*, 1113–1121. (g) Borin, A. C.; Serrano-Andrés, L.; Ludwig, V.; Coutinho, K.; Canuto, S. *Int. J. Quantum Chem.* **2006**, *106*, 2564–2577. (h) Hardman, S. J. O.; Thompson, K. C. *Biochemistry* **2006**, *45*, 9145–9155. (i) Seefeld, K. A.; Plützer, C.; Löwenich, D.; Häber, T.; Linder, R.; Kleinermanns, K.; Tatchen, J.; Marian, C. M. *Phys. Chem. Chem. Phys.* **2005**, *7*, 3021–3026. (j) Larsen, O. F. A.; van Stokkum, I. H. M.; Groot, M.-L.; Kennis, J. T. M.; van Grondelle, R.; van Amerongen, H. *Chem. Phys. Lett.* **2003**, *371*, 157–163. (l) Rachofsky, E. L.; Ross, J. B. A.; Krauss, M.; Osman, R. *J. Phys. Chem. A* **2001**, *105*, 190–197. (m) Jean, J. M.; Hall, K. B. *J. Phys. Chem. A* **2000**, *104*, 1930–1937. (n) Holmén, A.; Nordén, B.; Albinsson, B. *J. Am. Chem. Soc.* **1997**, *119*, 3114–3121. (o) Evans, K.; Xu, D.; Kim, Y.; Nordlund, T. M. *J. Fluoresc.* **1992**, *2*, 209–216.

(15) D'Souza, F.; Gadde, S.; Islam, D.-M. S.; Pang, S.-C.; Schumacher, A. L.; Zandler, M. E.; Horie, R.; Araki, Y.; Ito, O. *Chem. Commun.* **2007**, 480–482.

(16) (a) Meier, H. *Angew. Chem., Int. Ed.* **2005**, *44*, 2482–2506. (b) Gompper, R.; Wagner, H.-U. *Angew. Chem., Int. Ed. Engl.* **1988**, *27*, 1437–1455.

(17) Recent examples involving small molecules oligomers Davies, J. A.; Elangovan, A.; Sullivan, P. A.; Olbricht, B. C.; Bale, D. H.; Ewy, T. R.; Isborn, C. M.; Eichinger, B. E.; Robinson, B. H.; Reid, P. J.; Li, X.; Dalton, L. R. *J. Am. Chem. Soc.* **2008**, *130*, 10565–10575. (b) Jordan, B. J.; Pollier, M. A.; Ofir, Y.; Joubanian, S.; Mehtala, J. G.; Sinkel, C.; Caldwell, S. T.; Kennedy, A.; Rabani, G.; Cooke, G.; Rotello, V. M. *Chem. Commun.* **2008**, 1653–1655. (c) Ortíz, A.; Insuasty, B.; Torres, M. R.; Herranz, M. A.; Martín, N.; Viruela, R.; Ortí, E. *Eur. J. Org. Chem.* **2008**, 99–108. (d) Zhou, Y.; Xiao, Y.; Chi, S.; Qian, X. *Org. Lett.* **2008**, *10*, 633–636. (e) Yamaguchi, Y.; Shimoi, Y.; Ochi, T.; Wakamiya, T.; Matsubara, Y.; Yoshida, Z-i *J. Phys. Chem. B* **2008**, *112*, 5074–5084. (f) Khrarnov, D. M.; Bielawski, C. W. *J. Org. Chem.* **2007**, *72*, 9407–9417. (g) Yuan, M.-S.; Liu, Z.-Q.; Fang, Q. *J. Org. Chem.* **2007**, *72*, 7915–7922. (h) Meier, H.; Mühling, B.; Gerold, J.; Jacob, D.; Oehlhof, A. *Eur. J. Org. Chem.* **2007**, 625–631. (i) Dufresne, S.; Bourgeaux, M.; Skene, W. G. *J. Mater. Chem.* **2007**, *17*, 1166–1177. (j) Sakai, N.; Sisson, A. L.; Bhosale, S.; Fürstenberg, A.; Banerji, N.; Vauthey, E.; Matile, S. *Org. Biomol. Chem.* **2007**, *5*, 2560–2563. (k) Oliva, M. M.; Casado, J.; Raposo, M. M. M.; Fonseca, A. M. C.; Hartmann, H.; Hernández, V.; Navarrete, J. T. L. *J. Org. Chem.* **2006**, *71*, 7509–7520. (l) Lu, Z.; Lord, S. J.; Wang, H.; Moerner, W. E.; Twieg, R. J. *J. Org. Chem.* **2006**, *71*, 9651–9657. (m) Sonoda, Y.; Goto, M.; Tsuzuki, S.; Tamaoki, N. *J. Phys. Chem. A* **2006**, *110*, 13379–13387. (n) Lin, J.-H.; Elangovan, A.; Ho, T.-I. *J. Org. Chem.* **2005**, *70*, 7397–7407. (o) Andersson, A. S.; Qvortrup, K.; Torbensen, E. R.; Mayer, J.-P.; Gisselbrecht, J.-P.; Boudon, C.; Gross, M.; Kadziola, A.; Kilså, K.; Nielsen, M. B. *Eur. J. Org. Chem.* **2005**, 3660–3671. (p) Murase, T.; Fujita, M. *J. Org. Chem.* **2005**, *70*, 9269–9278. (q) Sumalekshmy, S.; Gopidas, K. R. *J. Phys. Chem. B* **2004**, *108*, 3705–3712.

(18) (a) Bureš, F.; Schweizer, W. B.; Boudon, C.; Gisselbrecht, J.-P.; Gross, M.; Diederich, F. *Eur. J. Org. Chem.* **2008**, 994–1004. (b) Bureš, F.; Schweizer, W. B.; May, J. C.; Boudon, C.; Gisselbrecht, J.-P.; Gross, M.; Biaggio, I.; Diederich, F. *Chem. Eur. J.* **2007**, *13*, 5378–5387. (c) Michinobu, T.; Boudon, C.; Gisselbrecht, J.-P.; Seiler, P.; Frank, B.; Moonen, N. N. P.; Gross, M.; Diederich, F. *Chem. Eur. J.* **2006**, *12*, 1889–1905. (d) Moonen, N. N. P.; Pomerantz, W. C.; Gist, R.; Boudon, C.; Gisselbrecht, J.-P.; Kawai, T.; Kishioka, A.; Gross, M.; Irie, M.; Diederich, F. *Chem. Eur. J.* **2005**, *11*, 3325–3341.

(19) (a) Spitler, E. L.; Haley, M. M. *Org. Biomol. Chem.* **2008**, *6*, 1569–1576. (b) Spitler, E. L.; Monson, J. M.; Haley, M. M. *J. Org. Chem.* **2008**, *73*, 2211–2223. (c) Marsden, J. A.; Miller, J. J.; Shirtcliff, L. D.; Haley, M. M. *J. Am. Chem. Soc.* **2005**, *127*, 2464–2476.

(20) Preliminary results have been published: Butler, R. S.; Myers, A. K.; Bellarmine, P.; Abboud, K. A.; Castellano, R. K. *J. Mater. Chem.* **2007**, *17*, 1863–1865.

Table 1. Yields for the Preparation of Bromides **6** and Donor−Acceptor Purines **1** and **2**[a]

			yield (%)[b]		
derivative	R^1	R^2	**6**	**1**	**2**
a	NH_2	H	24	80	60
b	$NHCH_3$	H	55	26	73
c	$N(CH_3)_2$	H	80	39	71
d	NH_2	OBn[c]	77	42	82
e	NH_2	$N(CH_3)_2$	78	91	86
f	$N(CH_3)_2$	NH_2	68	77	75
g	$N(CH_3)_2$	$N(CH_3)_2$	89	93	64

[a] The syntheses of derivatives a, d, e, and f have been reported in ref 20. [b] Isolated yields shown. [c] Bn = benzyl.

"weak" acceptor group maintain high (>80%) quantum yields over a range of solvent polarities. Preparation of **3** through conventional amide-bond forming reactions (i.e., DCC coupling) underlies an attractive strategy for introduction of the fluorophores to peptidic architectures or for their connection to other molecules or surfaces. Overall, the work presents (a) the straightforward extension of the "push−pull" concept to purines to afford useful photophysical properties and (b) fundamental insight, from structure−property studies, prerequisite for the broader application of purines in biosensing and materials.

Results and Discussion

Synthesis of Donor−Acceptor Purines 1 and 2. The donor−acceptor purines (Figure 1 and Table 1) are accessible from a common intermediate, 2-amino-9-benzyl-6-chloropurine, **4**, made from benzylation of commercially available (or readily made[21]) 2-amino-6-chloropurine.[22] The benzyl group at N(9) serves as a protecting and solubilizing group (for organic solvents), and to impart tautomeric stability. Hydrogenolysis of **4** provides **5a** (see Table 1 for derivative letter codes);[23] subsequent diazotization and chlorination gives known 9-benzyl-2-chloropurine (not shown),[24] precursor to 2-methylamino **5b**[25] and 2-dimethylamino **5c** that are formed upon appropriate nucleophilic aromatic substitution (see the Supporting Information for synthetic details). DABCO-catalyzed alcoholysis or direct amination of **4** affords **5d**[26] and **5e**,[27] respectively. Finally, diazotization and chlorination of **4** gives 9-benzyl-2,6-dichloropurine (not shown), and access to **5f** (in two additional steps) and **5g** (in one additional step) (Scheme 1).

With the donor groups installed, the C(8) position is available for acceptor group introduction. The cyano group was selected due to its standard use in simple donor-π-acceptor molecules,[16−19] known introduction to halopurines through displacement[28] or metal-mediated cross-coupling reactions,[29] and amenability to further functionalization. Bromination at the C(8) position of **5** was accomplished with Br_2[25] to afford intermediates **6** in generally high yields (Table 1). The bromides were subsequently converted to their corresponding nitriles **1** using Gundersen's cyanation conditions ($Zn(CN)_2$, $Pd(PPh_3)_4$, NMP) in moderate yields and with good reproducibility.[29b] Several precautions seem to improve the outcome of the reactions including (a) degassing and drying the solvent (NMP), (b) slow addition of a $Zn(CN)_2$ solution to an already prepared purine/Pd mixture (see the Supporting Information for details) in an attempt to keep the concentration of excess cyanide low,[30] and (c) use of significant excesses of purified $Pd(PPh_3)_4$ (20−50 mol %) given what are likely highly coordinating purine species. While other Pd catalysts can be used, we and others[29a,b] have found that $Pd(PPh_3)_4$ is generally reliable. Finally, conversion of the nitriles **1** to carboxymethyl esters **2** comes in generally good yield through treatment with methanolic ammonia and then acidic hydrolysis of the intermediate methyl imidates (not shown).[28c] Worth noting, other (more direct) approaches to 8-carboxyesters **2** are conceivable. Among these, we have found that lithiation[31] or lithium−halogen exchange[32] followed by an electrophilic quench (e.g., with methyl chloroformate) are impractically capricious for substrates **5**.

Scheme 1. Synthesis of Donor−Acceptor Purines **1** and **2**

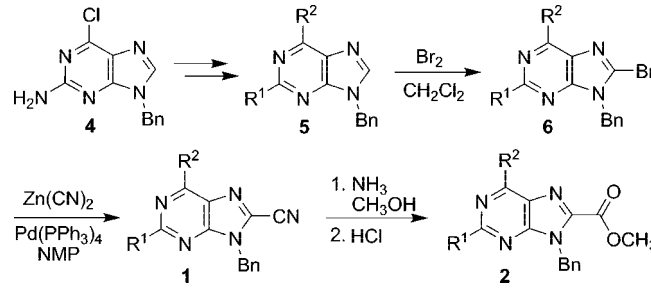

Design and Synthesis of Carboxamides 3. Given access to **1** and **2**, we envisioned that an amide linkage at the C(8) position could mutually serve as an electron-accepting function and the basis for later connecting the purines to biomolecules or surfaces. Along these lines, while access to primary ($CONH_2$) and simple tertiary (e.g., $CON(CH_3)_2$)[28c,31,33] amides is reasonably well-described for purines, routes to diverse amides (including secondary amides) are largely limited to the palladium-catalyzed carboxyamidation chemistry of Eaton and co-workers (reagents/conditions: 8-bromopurine, amine, CO (50 psi), $Pd(PPh_3)_4$, NEt_3,

(21) Igi, M.; Hayashi, T. Process for preparing 2-amino-6-halopurines and intermediates. EP 543095, 1993.
(22) Holý, A.; Günter, J.; Dvoráková, H.; Masojídková, M.; Andrei, G.; Snoeck, R.; Balzarini, J.; De Clercq, E. *J. Med. Chem.* **1999**, *42*, 2064–2086.
(23) Liu, F.; Dalhus, B.; Gundersen, L.-L.; Rise, F. *Acta Chem. Scand.* **1999**, *53*, 269–279.
(24) Tobrman, T.; Dvorák, D. *Org. Lett.* **2006**, *8*, 1291–1294.
(25) Kurimoto, A.; Ogino, T.; Ichii, S.; Isobe, Y.; Tobe, M.; Ogita, H.; Takaku, H.; Sajiki, H.; Hirota, K.; Kawakami, H. *Bioorg. Med. Chem.* **2003**, *11*, 5501–5508.
(26) Linn, J. A.; McLean, E. W.; Kelley, J. L. *J. Chem. Soc., Chem. Commun.* **1994**, 913–914.
(27) Martin, A. M.; Butler, R. S.; Ghiviriga, I.; Giessert, R. E.; Abboud, K. A.; Castellano, R. K. *Chem. Commun.* **2006**, 4413–4415.
(28) (a) Butora, G.; Schmitt, C.; Levorse, D. A.; Streckfuss, E.; Doss, G. A.; MacCoss, M. *Tetrahedron* **2007**, *63*, 3782–3789. (b) Ho, C. Y.; Kukla, M. J. *Bioorg. Med. Chem. Lett.* **1991**, *1*, 531–534. (c) Kato, T.; Arakawa, E.; Ogawa, S.; Suzumura, Y.; Kato, T. *Chem. Pharm. Bull.* **1986**, *34*, 3635–3643. (d) Matsuda, A.; Nomoto, Y.; Ueda, T. *Chem. Pharm. Bull.* **1979**, *27*, 183–192.
(29) (a) Doláková, P.; Masojídková, M.; Holý, A. *Heterocycles* **2007**, *71*, 1107–1115. (b) Gundersen, L.-L. *Acta Chem. Scand.* **1996**, *50*, 58–63. (c) Nair, V.; Purdy, D. F. *Tetrahedron* **1991**, *47*, 365–382. (d) Tanji, K.; Higashino, T. *Heterocycles* **1990**, *30*, 435–440.
(30) The sensitivity of Pd catalysts to excess cyanide is well documented: (a) Erhardt, S.; Grushin, V. V.; Kilpatrick, A. H.; Macgregor, S. A.; Marshall, W. J.; Roe, D. C. *J. Am. Chem. Soc.* **2008**, *130*, 4828–4845. (b) Chidambaram, R. *Tetrahedron Lett.* **2004**, *45*, 1441–1444. (c) Marcantonio, K. M.; Frey, L. F.; Liu, Y.; Chen, Y.; Strine, J.; Phenix, B.; Wallace, D. J.; Chen, C.-y. *Org. Lett.* **2004**, *6*, 3723–3725. (d) Sundermeier, M.; Mutyala, S.; Zapf, A.; Spannenberg, A.; Beller, M. *J. Organomet. Chem.* **2003**, *684*, 50–55.
(31) Hayakawa, H.; Haraguchi, K.; Tanaka, H.; Miyasaka, T. *Chem. Pharm. Bull.* **1987**, *35*, 72–79.
(32) Công-Danh, N.; Beaucourt, J.-P.; Pichat, L. *Tetrahedron Lett.* **1979**, 2385–2388.
(33) Gudmundsson, K. S.; Daluge, S. M.; Condreay, L. D.; Johnson, L. C. *Nucleosides, Nucleotides Nucleic Acids* **2002**, *21*, 891–901.

Scheme 2. Synthesis of Purinyl Carboxamides **3**

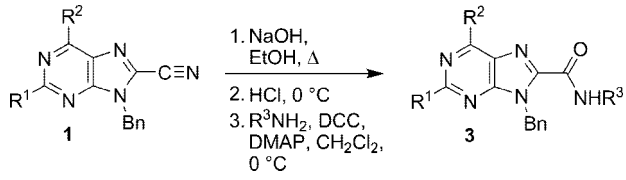

Table 2. Yields for the Preparation of Carboxamides **3**

entry	product	R^1	R^2	R^3	yield (%)[a]
1	**3g1**	$N(CH_3)_2$	$N(CH_3)_2$	$(CH_2)_3CH_3$	42
2	**3g2**	$N(CH_3)_2$	$N(CH_3)_2$	$CH_2CO_2CH_3$	82
3	**3g3**	$N(CH_3)_2$	$N(CH_3)_2$	$(CH_2)_4CO_2CH_3$	45
4	**3f**	$N(CH_3)_2$	NH_2	$CH_2CO_2CH_3$	51

[a] Isolated yields shown.

and DMF).[34,35] Eaton's approach could, in theory, be entertained beginning from bromides **6**. We chose to alternatively explore amide preparation via the intermediate (and generally unstable[28c,d,36]) 8-carboxypurine (generated from hydrolysis of either **1** or **2**) using appropriate amines and *standard peptide coupling conditions*.

Four examples (Scheme 2 and Table 2) illustrate the approach. Hydrolysis of bis(dimethylamino) derivative **1g** using 10% aqueous sodium hydroxide in ethanol first provides the carboxylate salt (not shown), an apparently stable species that does not require special handling or storage. Following protonation with HCl at 0 °C, the carboxylic acid is kept cold and used immediately[37] in a DCC-mediated coupling reaction with various primary amines. Entry 1 shows the result using simple butylamine,[38] while entries 2−4 that use the methyl esters of glycine and 5-aminovaleric acid are more relevant to incorporation of the purines within peptide sequences. Entry 4 further shows, expectedly, that the aromatic amino group at C(6) is relatively non-nucleophilic under these conditions.

X-ray Crystallographic Analysis. The X-ray crystal structures of ester **2f** and amide **3f** are presented in Figure 2 (additional crystallographic data, including ORTEP plots, are presented in the Supporting Information), as they highlight some of the features common to the donor−acceptor purines in the solid state. The structures of two nitriles, isomers **1e** and **1f**, have already been reported.[20] At the molecular level, the donor and acceptor substituents are fully conjugated with the purine cores. The dimethylamino groups are planar (sum of the three C−N−C bond angles = 360°) and the nonhydrogen atoms defining the methyl ester (Figure 2a) or amide (Figure 2b) substituents deviate from the mean purine plane by <0.1 Å. The −NH of the amide group of **3f** is expectedly positioned on the same side as N(7), a consequence of electrostatics (N(7)···N(16) = 2.74 Å). Finally, important for how the purines arrange in the solid state, the geometries of the N(9) benzyl substituents can be analyzed through two torsion angles, ∠*abcd* and ∠*bcde* (labeled in Figure 2a). For all four structures (**1e**, **1f**, **2f**, and **3f**) the phenyl and purine planes are nearly perpendicular (∠*abcd* = 82°, 91°, 103°, and 89°, respectively) while the values for ∠*bcde* vary as the phenyl group responds to nearest neighbors in the solid state.[39]

Key aspects of the packing structures of **2f** and **3f** are shown (Figure 2). Ester **2f**, like **1f**, forms H-bonded dimers from its Hoogsteen edge (Figure 2a), but through four hydrogen bonds (N(7)···N(10)′ = 3.03 Å; O(15)···N(10)′ = 2.87 Å) instead of two.[40] The structure is reminiscent of other quadruply H-bonded dimers derived from purines.[26,27,41] Amide **3f** (Figure 2b) instead forms infinite polar chains via intermolecular H-bonding between amide carbonyl oxygens and amino group hydrogens (N(10)···O(15)′ = 2.97 Å). This pattern bears relevance to the "guanine ribbons" exploited by Gottarelli and co-workers, the intrinsic dipole of which has been shown critical to gel and liquid crystal formation and electronic device performance.[4] Ester **2f** additionally shows (Figure 2a) strong antiparallel (dipolar) π-stacking interactions (interplanar distance = 3.30 Å), documented previously for **1e** (3.32 Å) and **1f** (3.38 Å),[20] and common for donor−acceptor molecules.[19a,c,42,43] Within this motif the ester acceptor of one molecule is positioned directly above the pyrimidine ring of a neighboring purine; the same ester-pyrimidine packing can be found in the structure of **3f**. Extended packing diagrams are provided in the Supporting Information that reveal the role of the benzyl substituents in the longer-range organization of the molecules. Most importantly, the crystal structures highlight relationships between the built-in molecular recognition functionality of the purines and their solid-state organization; this knowledge could potentially be used to optimize device performance and optoelectronic properties.

Absorption Properties. In general, the photophysical properties of 2-amino- and 2-dimethylaminopurine derivatives remain intensely studied, from both mechanistic and applied perspectives (vide infra). In solution, the optical behavior of various C(8)-unsubstituted compounds has been evaluated in water,[9c,44] but equivalently comprehensive measurements in organic media are mostly restricted to unsubstituted 2-aminopurines[9c,14b,o,44a,b] and 2-dialkylaminopurines.[44a,b] Relevant data from these compounds and **5** are discussed in the context of the donor−acceptor purines **1**−**3** below. The basic premise is that knowing the solvent-induced absorption and emission changes for **1**−**3** and understanding the dependence of the changes on structure should expose opportunities for the molecules in both biological and materials applications. Discussion of the absorption and emission

(34) Tu, C.; Keane, C.; Eaton, B. *Nucleosides Nucleotides* **1997**, *16*, 227–237.
(35) There are, however, no examples of C(8) purinyl carboxamides where C(2) is substituted with an NR′R″ group.
(36) Naka, T.; Honjo, M. *Chem. Pharm. Bull.* **1976**, *24*, 2052–2056.
(37) The putative acid formed upon hydrolysis of **1a** readily decarboxylates at room temperature in solution or the solid state; the process can be observed by TLC and ^{1}H NMR.
(38) Also tested was conversion of the carboxylic acid first to its acid chloride ($SOCl_2$, 80 °C, 1 h) and then to the amide (butylamine, NEt_3, THF, rt). The overall yield for the two-step process was a lower 23%.
(39) A comparison of the bond lengths for **1e**, **1f**, **2f**, **3f**, and 2-AP is presented in Table S2 (Supporting Information). The values agree within ~0.05 Å.
(40) The compound at best only weakly dimerizes in $CDCl_3$; poor solubility at high concentrations (e.g., 10 mM) has prevented a more detailed analysis.
(41) (a) Ong, H. C.; Zimmerman, S. C. *Org. Lett.* **2006**, *8*, 1589–1592. (b) Park, T.; Todd, E. M.; Nakashima, S.; Zimmerman, S. C. *J. Am. Chem. Soc.* **2005**, *127*, 18133–18142. (c) Nowick, J. S.; Chen, J. S.; Noronha, G. *J. Am. Chem. Soc.* **1993**, *115*, 7636–7644.
(42) (a) Boiadjiev, S. E.; Lightner, D. A. *J. Org. Chem.* **2005**, *70*, 688–691. (b) Moonen, N. N. P.; Gist, R.; Boudon, C.; Gisselbrecht, J.-P.; Seiler, P.; Kawai, T.; Kishioka, A.; Gross, M.; Irie, M.; Diederich, F. *Org. Biomol. Chem.* **2003**, *1*, 2032–2034.
(43) (a) Yao, S.; Beginn, U.; Gress, T.; Lysetska, M.; Würthner, F. *J. Am. Chem. Soc.* **2004**, *126*, 8336–8348. (b) Würthner, F.; Yao, S.; Debaerdemaeker, T.; Wortmann, R. *J. Am. Chem. Soc.* **2002**, *124*, 9431–9447. (c) Würthner, F.; Yao, S. *Angew. Chem., Int. Ed.* **2000**, *39*, 1978–1981.
(44) (a) Smagowicz, J.; Wierzchowski, K. L. *J. Lumin.* **1974**, *8*, 210–232. (b) Drobnik, J.; Augenstein, L. *Photochem. Photobiol.* **1966**, *5*, 83–97. (c) Mason, S. F. *J. Chem. Soc.* **1954**, 2071–2081.

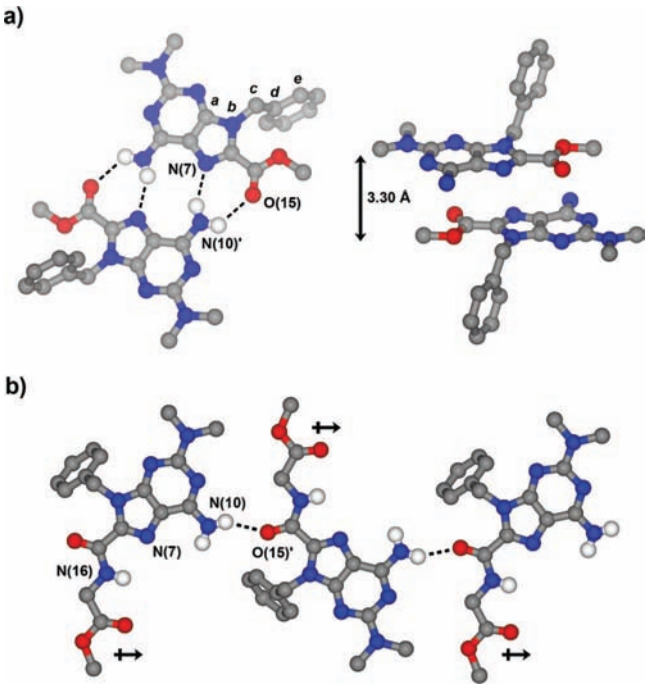

Figure 2. X-ray crystal structures of **2f** (a) and **3f** (b). (a) Dimers of **2f** formed by quadruple H-bonding (left) and antiparallel dipolar π-stacking (right). (b) Polar 1-D H-bonded chains of **3f** in the solid state. H-bonding interactions are indicated by dashed lines. Some hydrogens have been omitted for clarity. Additional crystallographic details are provided in the Supporting Information.

Table 3. Electronic Absorption and Emission Data for **1**−**3** in CH_2Cl_2[a]

purine	lowest energy abs λ_{max} [nm] (log ε [M^{-1} cm^{-1}])	em λ_{max} [nm][b]	$\Delta\lambda_{max}$	Φ_F[c]
1a[d]	326 (3.2)	371	45	0.20
1b	341 (3.8)	383	41	0.58
1c	361 (4.2)	429	68	0.90
1d[d]	311 (4.3)	355	44	0.81
1e[d]	324 (4.2)	375	51	0.30
1f[d]	336 (4.1)	387	51	>0.95
1g	348 (4.4)	388	40	0.20
2a[d]	328 (4.1)	379	51	0.42
2b	345 (3.2)	403	58	0.65
2c	362 (4.1)	433	71	0.81
2d[d]	315 (4.3)	371	56	>0.95
2e[d]	330 (4.2)	393	63	>0.95
2f[d]	338 (4.1)	409	71	>0.95
2g	351 (4.3)	409	58	0.90
3g1	338 (4.2)	402	64	0.87
3g2	343 (4.3)	407	64	0.91

[a] All measurements performed at room temperature. [b] All experiments were performed using optical densities ≤0.1 at the excitation wavelength (λ_{ex} = 320 nm; for **3g1** and **3g2** λ_{ex} = 360 nm). [c] Fluorescence quantum yields are relative to the quantum yield of quinine sulfate in 0.1 M H_2SO_4 (Φ_F = 0.577). [d] Data previously reported in ref 20.

data will each begin with the behavior of **1**−**3** in dichloromethane (CH_2Cl_2), followed by solvatochromic studies.

Absorption data for **1**−**3** in CH_2Cl_2 is provided in Table 3 and graphically for the **g** series in Figure 3; all tabular data for the C(8)−H purines **5** is presented in the Supporting Information. The absorption spectra of **5** show two intense low-energy bands at ∼250 and ∼300 nm; both absorption bands are red-shifted for **1**−**3** (Figure 3). By analogy to 2-AP and 2-amino-

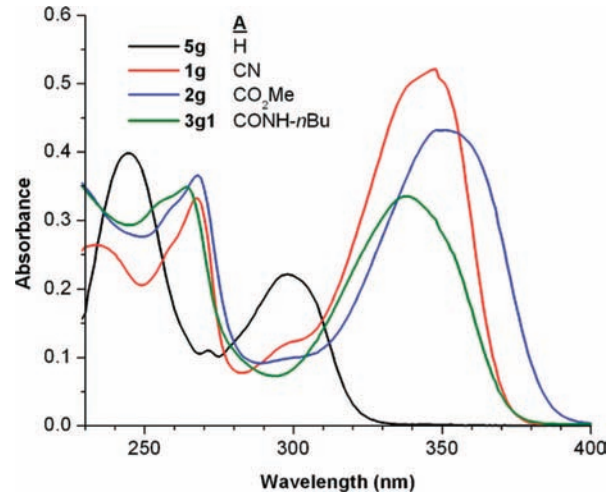

Figure 3. Absorption data for the 2,6-bis(dimethylamino)purine series **g** in CH_2Cl_2 (2×10^{-5} M).

9-methylpurine,[14d,m,44a,45] and verified by preliminary calculations (vide infra), we assign the lowest energy band to the $^1(\pi\pi^*$ $L_a)$[46] transition ($S_0 \rightarrow S_1$), and the higher-energy band to the $^1(\pi\pi^*$ $L_b)$ transition ($S_0 \rightarrow S_3$).[47] In all cases the maximum absorption wavelengths (λ_{max}) are concentration independent over a typical range for the measurements (5−60 μM) and plots of absorbance versus concentration for the low-energy band are linear. Moreover, the extinction coefficients are moderately high (log $\varepsilon \approx 4$), consistent with other 2-AP derivatives.[14n,44c]

The remaining results and discussion will focus primarily on the low-energy absorption for **5** and **1**−**3** since it leads to fluorescence emission. Earlier optical and theoretical studies[9d,14m,n,44] with purines help to rationalize the response of this band first to donor structure at C(2) and C(6), and then to acceptor substitution at C(8). The low-energy transition moment ($S_0 \rightarrow S_1$, $\pi \rightarrow \pi^*$) for 2-amino-9-methylpurine is polarized at an angle ∼55° with respect to the purine C(4)−C(5) bond (in the direction of N(1); Figure 1), a value relatively insensitive to "inert" substituents at N(9).[14n] Donor substituents at C(2), positioned ∼30° from the long axis (∼65° from the transition dipole moment) significantly affect this transition. Data from the acceptor-free purines **5** are illustrative (see Table S3). Purines **5a**−**5c**, for example, bearing donors *only* in the C(2) position, show the most red-shifted low-energy absorption bands whose wavelength scales with the donor ionization potential (NH_2 (304 nm) < $NHCH_3$ (317 nm) < $N(CH_3)_2$ (330 nm)). The presence of a donor at C(6) incidentally blue shifts the low-energy absorption wavelength ∼20−30 nm. The hypsochromic shift magnitude is relatively insensitive to the nature of the C(6) donating group such that the nature of the C(2) donor tunes the abs λ_{max}.

The introduction of acceptor substituents to C(8), on the purine long axis, significantly affects the absorption maxima (Figure 3); in general, the low-energy absorption band is red-shifted by 20−50 nm (and the higher-energy absorption band significantly less). Here, presumably, the transition dipole direction is further aligned with the purine long axis. The

(45) The optical behavior of the purines is relatively insensitive to the N(9) substituent. See refs 20 and 14o.
(46) For nomenclature, see:(a) Platt, J. R. *J. Chem. Phys.* **1949**, *17*, 484–495.
(47) Not discussed here is the n $\rightarrow \pi^*$ ($S_0 \rightarrow S_2$) transition that is weak and found at an intermediate energy. See ref 14 for details.

Table 4. Electronic Absorption and Emission Data for **1**−**3** in 1,4-Dioxane[a]

purine	lowest energy abs λ_{max} [nm] (log ε [M^{-1} cm^{-1}])	em λ_{max} [nm][b]	$\Delta\lambda_{max}$	Φ_F[c]
1a	331 (4.2)	381	50	0.34
1b[d]	342 (4.0)	390	48	0.61[d]
1c	355 (4.4)	424	69	0.91
1d	313 (4.3)	362	49	0.73
1e	334 (4.4)	373	39	0.78
1f	339 (4.2)	382	43	0.92
1g	345 (4.3)	383	38	>0.95
2a	331 (4.2)	386	55	0.64
2b	345 (4.1)	405	60	0.65
2c	358 (4.2)	426	68	0.83
2d	313 (4.3)	376	63	>0.95
2e	334 (4.3)	391	57	>0.95
2f	340 (4.4)	399	59	>0.95
2g	344 (4.3)	402	58	>0.95
3g1	332 (4.2)	392	60	>0.95
3g2	336 (4.3)	397	61	>0.95

[a] All measurements performed at room temperature. [b] All experiments were performed using optical densities ≤0.1 at the excitation wavelength (λ_{ex} = 320 nm; for **3g1** and **3g2** λ_{ex} = 360 nm). [c] Fluorescence quantum yields are relative to the quantum yield of quinine sulfate in 0.1 M H_2SO_4 (Φ_F = 0.577). [d] Decomposition has been observed upon prolonged irradiation (vide infra).

Table 5. Electronic Absorption and Emission Data for **1**−**3** in Acetonitrile[a]

purine	lowest energy abs λ_{max} [nm] (log ε [M^{-1} cm^{-1}])	em λ_{max} [nm][b]	$\Delta\lambda_{max}$	Φ_F[c]
1a	330 (3.2)	381	51	0.31
1b	342 (3.0)	405	63	0.58
1c	357 (3.9)	440	83	0.53
1d	313 (4.3)	366	53	0.65
1e	326 (4.3)	378	52	0.08
1f	338 (4.3)	396	58	0.55
1g	344 (4.3)	394	50	0.26
2a	330 (4.3)	388	58	0.55
2b	345 (3.2)	413	68	0.66
2c	359 (4.1)	444	85	0.60
2d	316 (4.2)	382	66	0.87
2e	332 (4.4)	399	67	0.83
2f	342 (4.1)	414	72	0.75
2g	347 (4.3)	415	68	0.86
3g1	333 (4.2)	405	72	>0.95
3g2	336 (4.3)	409	73	>0.95

[a] All measurements performed at room temperature. [b] All experiments were performed using optical densities ≤0.1 at the excitation wavelength (λ_{ex} = 320 nm; for **3g1** and **3g2** λ_{ex} = 360 nm). [c] Fluorescence quantum yields are relative to the quantum yield of quinine sulfate in 0.1 M H_2SO_4 (Φ_F = 0.577).

maxima shifts are fairly similar among the acceptors chosen (**1g** = 348 nm; **2g** = 348 nm; **3g1** = 338 nm), consistent with acceptor group trends observed within other systems (λ_{max} CN ≈ λ_{max} CO_2CH_3 > λ_{max} $CONH_2$).[48] Noteworthy, the "parent" **a** series shows a red shift of ∼26 nm upon CN/CO_2CH_3 introduction (i.e., conversion of **5a** to **1a**/**2a**), a potentially useful improvement over 2-AP for selective excitation in biological settings.

Optical data for **1**−**3** in 1,4-dioxane, acetonitrile, and methanol (and H_2O for series **a**) is provided in Tables 4−6 to complement the CH_2Cl_2 data; tabular data for C(8)−H purines **5** is presented in the Supporting Information. The low-energy absorption maximum for the purines (collectively) is relatively

Table 6. Electronic Absorption and Emission Data for **1**−**3** in Methanol[a]

purine	lowest energy abs λ_{max} [nm] (log ε [M^{-1} cm^{-1}])	em λ_{max} [nm][b]	$\Delta\lambda_{max}$	Φ_F[c]
1a	333 (3.2)	398	65	0.64
1a[d]	331 (2.8)	406	75	0.88
1b[e]	342 (3.9)	417	75	0.49[e]
1c	358 (4.0)	456	98	0.14
1d	318 (4.1)	382	64	0.14
1e	327 (4.2)	389	62	0.01
1f	338 (4.2)	410	72	0.80
1g	342 (4.4)	403	61	0.03
2a	335 (4.1)	412	77	0.87
2a[d]	325 (4.1)	420	95	>0.95
2b	345 (3.9)	429	84	0.61
2c	362 (4.1)	466	104	0.17
2d	321 (4.3)	405	84	0.92
2e	331 (4.2)	420	89	0.39
2f	345 (4.1)	436	91	0.76
2g	347 (4.2)	432	85	0.66
3g1	335 (4.2)	424	89	0.89
3g2	340 (4.2)	429	89	0.90

[a] All measurements performed at room temperature. [b] All experiments were performed using optical densities ≤0.1 at the excitation wavelength (λ_{ex} = 320 nm; for **3g1** and **3g2** λ_{ex} = 360 nm). [c] Fluorescence quantum yields are relative to the quantum yield of quinine sulfate in 0.1 M H_2SO_4 (Φ_F = 0.577). [d] Measurements taken in water. [e] Decomposition has been observed upon prolonged irradiation (vide infra).

insensitive to the solvent polarity, only fluctuating by a few nanometers across the range of solvents. The result is similar to 2-AP[14l,o,44a] and reflects a small change in dipole moment magnitude and/or direction between the ground and Franck−Condon excited states. Again, plots of the optical density versus concentration for each compound in each solvent show linearity. That **1**−**3** do not appear to aggressively aggregate by dipolar π-stacking[42,43] can be partially attributed to their relatively modest ground-state dipole moments (μ_{gs} ≈ 2−6 D, vide infra).

Emission Properties in CH_2Cl_2. The electronic emission spectra for **1**−**3** are shown in Figure 4 and the data are summarized in Tables 3−6; data for **5** is provided in the Supporting Information. Irradiation at the low-energy absorption wavelength of C(8) unsubstituted 2-amino- and 2-dimethylaminopurines **5** in CH_2Cl_2 (Table S3), for example, yields a broad and featureless emission from 350−400 nm depending on the substitution pattern. The results are consistent with the limited data for purines in organic solvents.[9c,44a,49] The emission band is red-shifted by 14−36 nm upon conversion of **5** to **1**, and an additional 4−22 nm upon the nitrile's transformation to the methyl ester **2**. For parent series **a** (**5a**, **1a**, and **2a**), for example, the emission wavelengths increase from 357 → 371 → 379 nm; even larger changes are found across series **f** (360 → 387 → 409 nm). Exceptions to this progression are found only for conversion of **5b**, **5d**, and **5g** to **1**, where the emission maxima show a small hypsochromic shift (∼5 nm). The emission of amide **3g1** is slightly blue-shifted relative to ester **2g**. Although correlations between emission energies and parameters that reflect electron-acceptor strength (substituent electron affinity) are system dependent, these general trends have been observed in stilbene-like D−A systems.[48] For the donor−acceptor purines in CH_2Cl_2, the Stokes shifts are 40−71 nm and the values are generally highest for the esters **2** and amides **3**, suggesting a

(48) Anstead, G. M.; Carlson, K. E.; Kym, P. R.; Hwang, K.-J.; Katzenellenbogen, J. A. *Photochem. Photobiol.* **1993**, *58*, 785–794.

(49) Balu, N.; Gamcsik, M. P.; Colvin, M. E.; Colvin, O. M.; Dolan, M. E.; Ludeman, S. M. *Chem. Res. Toxicol.* **2002**, *15*, 380–387.

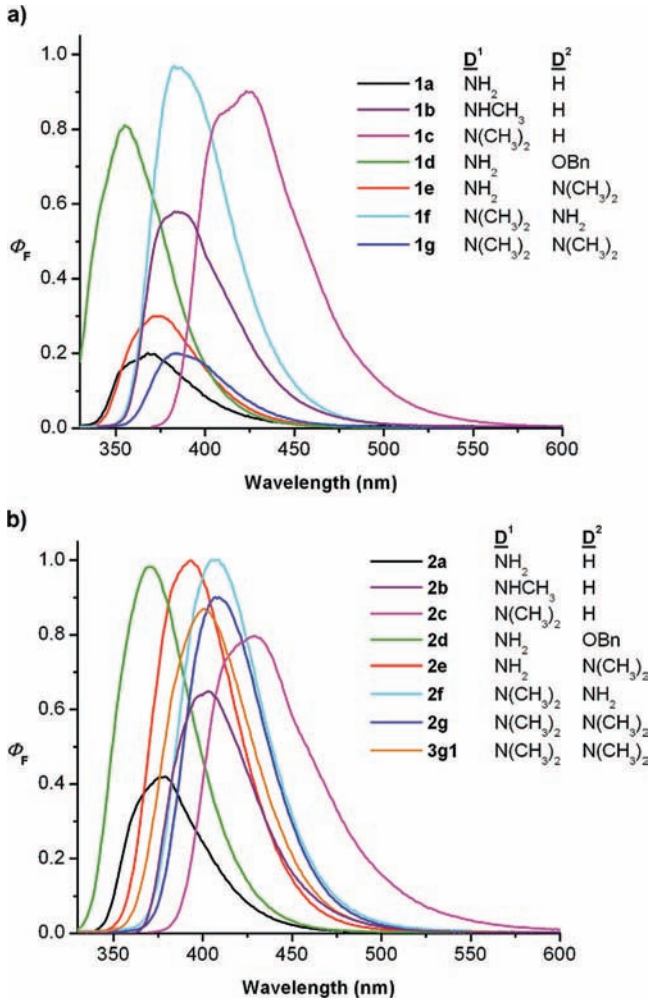

Figure 4. Normalized emission spectra (based on quantum yield) for **1** (a), **2**, and **3g1** (b) in CH_2Cl_2 (concentration = 5×10^{-6} M; λ_{ex} as indicated in Table 3).

greater degree of structural reorganization in the excited state for these compounds.

Quantum yields for **1**−**3** were determined using quinine sulfate in 0.1 M H_2SO_4 ($\Phi_F = 0.577$)[50] as a standard. In CH_2Cl_2, the quantum yields of **5** parallel what has been reported for 9-ethyl-2-aminopurine ($\Phi_F = 0.085$ in $CHCl_3$), 2-aminopurine, and 2-dimethylaminopurine in organic solvents.[9c,44a] The values are generally highest for purines bearing only a C(2) donor, and increase with the donor strength (**a** < **b** < **c**). Quantum yields are consistently low (≤12%) when a C(6) donor is present (again, the Φ_F values are vanishing in the *absence* of a donor at C(2)[9,51]). The addition of the C(8)−CN acceptor leads to dramatic quantum yield increases from **5**; compounds **1d** ($\Phi_F = 0.033 \rightarrow 0.81$), **1e** ($\Phi_F = 0.013 \rightarrow 0.30$), and **1g** ($\Phi_F = 0.033 \rightarrow 0.20$) show increases of *2 orders of magnitude* while the values for compounds **1c** and **1f** increase to near unity. Comparison of isomeric species **1e** ($\Phi_F = 0.30$) and **1f** ($\Phi_F = > 0.95$) highlights the contribution of the C(2) donor, and its position, to the quantum yield. Although the enhancements are considerably more modest across the **a** series, further conversion of the nitriles **1** to the methyl esters **2** serves to increase the quantum yields to *50% or higher across the board* (Table 3). High values also appear to characterize amides **3**. These trends are difficult to predict solely on the basis of optical energy gaps (vide infra) or apparent acceptor "strength". Finally, as shown for selected compounds before,[20] the fluorescence lifetimes (τ_F) determined in CH_2Cl_2 scale, in general, with the quantum yields and the best emitters have τ_F values of ∼2.5−4 ns (larger than 2-AP in 1,4-dioxane (1.5 ns)[14b]). All decays could be fit, with χ^2 values close to 1, to a single exponential, and are consistent with fluorescence emission from the lowest singlet excited state (S_1) (see the Supporting Information for additional data and experimental details).

Table 7. Change in Dipole from the Ground to Excited State ($\Delta\mu_{ge}$) Based on Plots of Stokes Shift versus E_T^N for **1**−**3**[a]

purine	*a* (Å)[b]	slope (cm^{-1})[c]	*R*[c]	$\Delta\mu_{ge}$[d]	slope (cm^{-1})[c]	*R*[c]	$\Delta\mu_{ge}$[d]
		including 1,4-dioxane data			excluding 1,4-dioxane data		
1a	4.0	2170	0.951	2.04	2720	0.999	2.29
1b	4.1	3260	0.902	2.60	4200	0.935	2.95
1c	4.2	2690	0.937	2.45	3390	0.968	2.75
1d	4.5	1880	0.882	2.27	2730	0.982	2.73
1e	4.2	2580	0.915	2.40	1590	0.954	1.88
1f	4.2	3070	0.996	2.61	2820	1.00	2.51
1g	4.4	2770	0.979	2.66	3120	0.983	2.83
2a	4.1	3330	0.952	2.63	4070	0.989	2.90
2b	4.2	2540	0.952	2.38	3270	0.997	2.70
2c	4.3	3060	0.978	2.70	3490	0.984	2.89
2d	4.6	2260	0.832	2.57	3630	0.997	3.26
2e	4.4	3350	0.984	2.93	3560	0.978	3.02
2f	4.3	2610	0.957	2.50	2190	0.930	2.29
2g	4.5	2730	0.949	2.73	3530	0.995	3.11
3g1	4.8	2930	0.984	3.12	3380	0.997	3.35

[a] See the Results and Discussion section for details. [b] Onsager radii corresponding to volumes determined by eq 2. See the text for details. [c] The slopes and correlation factors (*R*) for fitted lines from Stokes shift (cm^{-1}) versus E_T^N plots (see Figure 5 for examples). [d] Values determined using eq 1. See the text for details.

Fluorescence Solvatochromism. The emission properties for **5** and **1**−**3** have been evaluated in 1,4-dioxane ($E_T(30) = 36.0$ kcal mol^{-1}), CH_2Cl_2 ($E_T(30) = 40.7$ kcal mol^{-1}), acetonitrile ($E_T(30) = 45.6$ kcal mol^{-1}), methanol ($E_T(30) = 55.4$ kcal mol^{-1}), and additionally for the **a** series, water ($E_T(30) = 63.1$ kcal mol^{-1}).[52,53] The data are represented in Tables 3−7, Figures 5 and 6, and the Supporting Information. For the acceptor-bearing purines **1**−**3**, the emission wavelength maxima generally increase with increasing solvent polarity; the Stokes shifts correspondingly increase to the tune of 16−32 nm for **1**, 29−40 nm for **2**, and ∼30 nm for **3g** over the range of solvent polarities (from 1,4-dioxane to methanol or water). Thus, em λ_{max} ranges from 355 to 466 nm for the purines **1**−**3** depending on substitution pattern and solvent. Upon the suggestion of Tor and co-workers,[53a] we have used plots of the Stokes shift versus Reichardt's normalized microscopic solvent polarity parameter E_T^N (or equivalently, $E_T(30)$)[52] to compare the purines more quantitatively in terms of their solvent-dependent optical behavior (slopes for fitted lines are given in Table 7). The E_T^N polarity scale, unlike methods that use bulk solvent polarity functions such as the dielectric constant (ε) and refractive index (n), takes specific solvent−solute interactions into account. Even with notoriously anomalous dioxane[53c] and H-bonding solvents[54]

(50) Eastman, J. W. *Photochem. Photobiol.* **1967**, *6*, 55–72.
(51) Even when a dimethylamino group is at C(6): Albinsson, B. *J. Am. Chem. Soc.* **1997**, *119*, 6369−6375.
(52) Reichardt, C. *Chem. Rev.* **1994**, *94*, 2319–2358.
(53) (a) Sinkeldam, R. W.; Tor, Y. *Org. Biomol. Chem.* **2007**, *5*, 2523–2528. (b) Katritzky, A. R.; Fara, D. C.; Yang, H.; Tämm, K.; Tamm, T.; Karelson, M. *Chem. Rev.* **2004**, *104*, 175–198. (c) Suppan, P.; Ghoneim, N. *Solvatochromism*; The Royal Society of Chemistry: Cambridge, 1997.

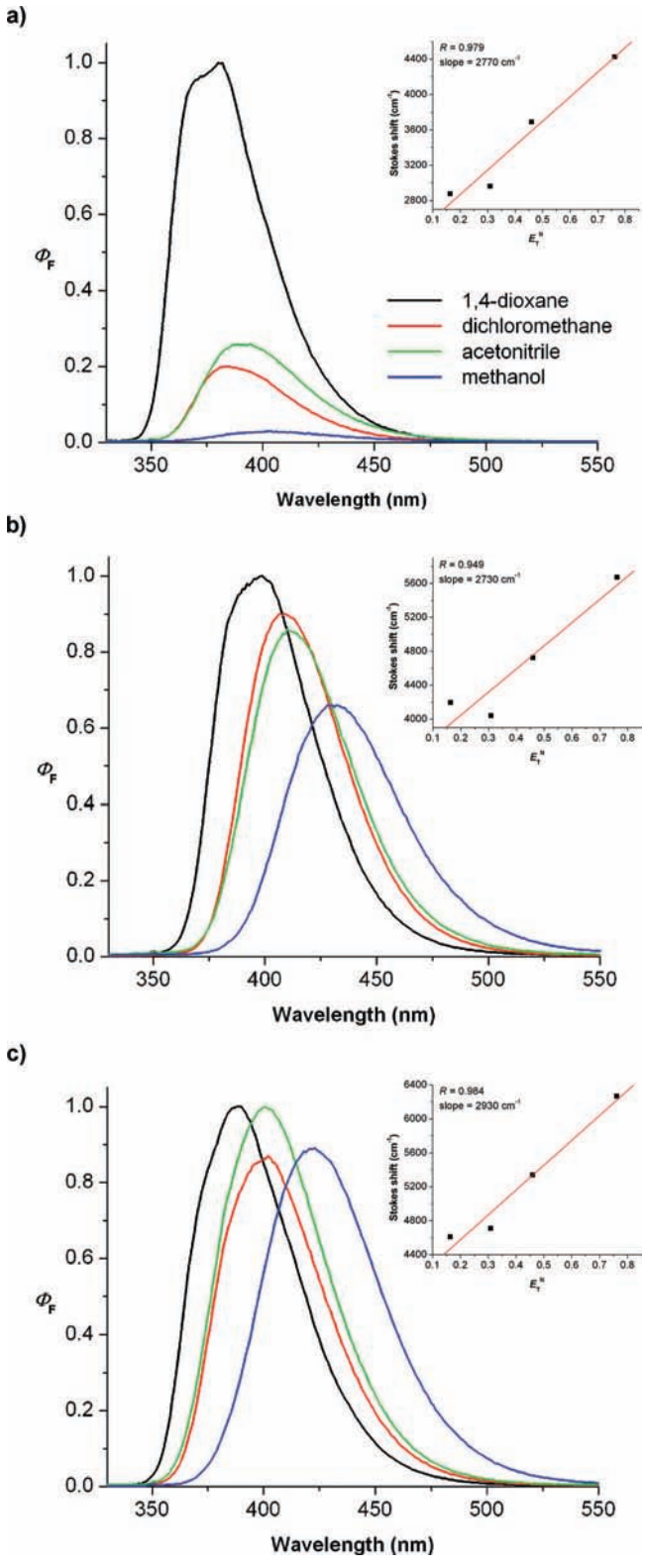

Figure 5. Normalized emission spectra (based on quantum yield) for **1g** (a), **2g** (b), and **3g1** (c) in various solvents (concentration = 5×10^{-6} M; λ_{ex} as indicated in Tables 3−6). The insets show plots of the Stokes shift (cm^{-1}) versus Reichardt's normalized solvent polarity measure, E_T^N. Solvent values are as follows. 1,4-dioxane = 0.164; dichloromethane = 0.309; acetonitrile = 0.460; methanol = 0.762; water = 1.000 (ref 52). See Table 7 for additional data.

like methanol (and water, for series **a**) included,[55] plots for **1a**−**g**, **2a**−**g**, and **3g1** give very good linear correlations

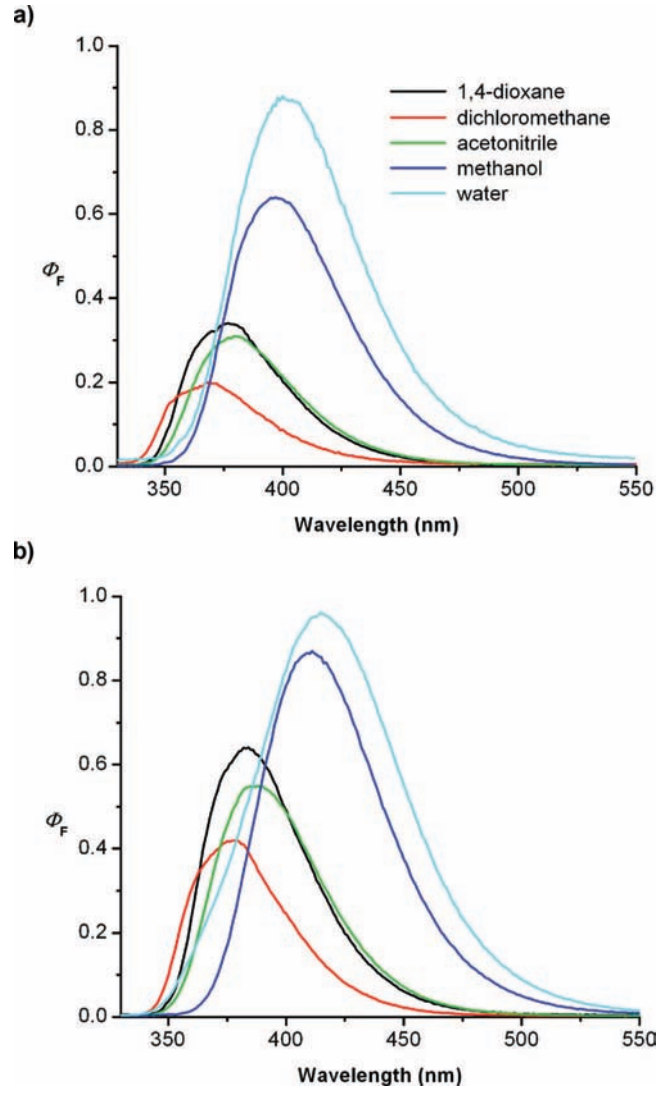

Figure 6. Normalized emission spectra (based on quantum yield) for **1a** (a) and **2a** (b) in various solvents (concentration = 5×10^{-6} M; λ_{ex} = 320 nm).

(average correlation factor, *R*, equals 0.94). The plots for the **g** series are given as insets in Figure 5. Removing the 1,4-dioxane data improves the **d** values substantially and boosts the overall average correlation factor to *0.98* (Table 7). Incidentally, plots of the Stokes shifts versus Δf (the orientation polarizability) show, on average, poor linear correlations as do Stokes shift versus E_T^N plots constructed using the data from acceptor-free **5**. Three important conclusions emerge from the studies: (a) The solvatochromic behavior is consistent with stabilization of an emissive excited-state that has polar character (i.e., $\mu_e > \mu_g$);[56] (b) the positive solvatochromic response is generally larger (based on the slopes) for the esters than the nitriles, consistent with some literature observations;[48] (c) given the usefulness of Stokes shift changes for sensing applications, purines **1**−**3** are importantly more responsive than the acceptor-free purines **5** or 2-AP due to their enhanced charge separation.

(54) Specific H-bonding interactions may (ref 14o) or may not (refs 14b and 14l) significantly influence 2-AP spectral shifts.
(55) Mannekutla, J. R.; Mulimani, B. G.; Inamdar, S. R. *Spectrochim. Acta, Part A* **2008**, *69*, 419–426.
(56) Lakowicz, J. R. *Principles of Fluorescence Spectroscopy*, 3rd ed.; Springer: New York, 2006.

The solvatochromic Stokes shift data could further be used to estimate the dipole moment change on excitation of the purines from the ground to excited-state using Samanta and Radhakrishnan's eq 1:[57]

$$\Delta\mu_{ge} = \mu_e - \mu_g = \sqrt{[(\text{slope} \times 81)/(11307.6 \times (6.2/a)^3]} \quad (1)$$

$$a(\text{in Å}) = \sqrt[3]{[(3 \times 1.33 \times v_w)/4\pi]} \quad (2)$$

The estimated $\Delta\mu_{ge}$ depends on a, the Onsager radius, the determination of which is notoriously difficult. Various protocols to estimate a are available in the literature;[58] for coumarin dyes, for example, the value has been taken as half the distance (in Å) between the donor amine nitrogen and acceptor carbonyl oxygen.[57a] We instead have used eq 2, where v_w is the calculated volume of the van der Waals surface created for each of **1**−**3** using Discovery Studio Visualizer v. 2.0 (Accelyrs Software, Inc.);[59] multiplying this volume by 1.33 approximates the molar volume in the liquid state.[58a,60] The structures used for the volume determinations (except **1d** and **2d**) could be produced directly in the program from atomic modifications of the crystal structure data presented earlier (for **1e**, **1f**, **2f**, and **3f**). For **1d** and **2d**, simple energy-minimized structures were used (MacroModel v. 9.1). The Onsager radii for the purines are given in Table 7 and fall between 4.0 and 4.8 Å. Worth noting, this method applied to PRODAN offers a value (4.0 Å) close to its accepted radius of 4.2 Å but gives a smaller value (3.2 Å) than the one generally used for 2-AP (3.8 Å).[14m,o,61] Together with the calculated slopes from the Stokes shift versus E_T^N plots, $\Delta\mu_{ge}$ values across 15 purines emerge between 2.0−3.1 D with 1,4-dioxane data included and 1.9−3.4 D without this data (Table 7). These values are (a) similar to experimental values for structurally related and extensively studied coumarin laser dyes,[55,57b] (b) consistent with the degree of charge separation suggested by theoretical analysis (vide infra), and (c) reasonable based on values already determined for 2-aminopurine experimentally[14a,o,44a,62] (e.g., 1.6,[44a] 2.8,[14o] 2.9 D[61b]) and computationally.[14a,f,l,m] Closer inspection reveals some expected trends, many of which have been identified earlier. The $\Delta\mu_{ge}$ values, for example, are, on average, larger for the esters **2** than the nitriles **1** within any one series.

The quantum yield values for donor−acceptor purines **1**−**3** generally decrease with increasing solvent polarity (Figure 5) *with the exception of series* **a**, which increases (Figure 6), and **b**, which is quite constant. The decrease in quantum yield with increasing polarity for donor−acceptor molecules is generally likened to stabilization of the polar excited state that introduces competing deactivation pathways.[56] There are some exceptions among **c**−**g** (e.g., **1f**), but the behavior shown in Figure 5a (for **1g**) is typical. Importantly, though, is that purines **1**−**3** do not respond equivalently to solvent polarity. The methyl esters **2** show only moderate decreases in fluorescence (see Figure 5b for **2g**), by comparison to **5** or **1**, as solvent polarity is increased; most derivatives even maintain high values regardless of the solvent. The same is true for amides **3** (see Figure 6c for **3g1**), the quantum yields of which remain near unity in all four solvents.

A notable and inversed quantum yield trend emerges within the "parent" **a** series (**5a**, **1a**, and **2a**), where the fluorescence efficiency increases as the solvent polarity is increased (Figure 6). For example, the quantum yield of **1a** increases from 0.34 in 1,4-dioxane to 0.88 in water (Figure 6a). The trend parallels what is known for 2-AP[9c,44a] and 2-amino-9-methylpurine,[62a] where less-efficient $\pi-\pi^*$ quenching by vibronic coupling to the $n-\pi^*$ state accompanies more polar solvents.[62a] Series **b** shows behavior between **a** and **c**, with reasonably high quantum yields across the range of solvent polarities. How this behavior is linked to the amino group (vide supra), for example through hydrogen bonding or excited-state pyramidalization, is currently unclear.

Chemical and Photochemical Stability. Purines **1**−**3** show no significant decomposition by TLC or ^{1}H NMR analysis after months of being stored as solids in vials or in solutions of 1,4-dioxane, dichloromethane, acetonitrile, or methanol with exposure to air and ambient light. The photochemical stability of **5a**, **5b**, **1a**, **1b**, **1g**, and **2b** was further evaluated in nondegassed CH_2Cl_2 by monitoring the fluorescence intensity (at em λ_{max}) during constant irradiation (**5a** and **5b**: λ_{ex} = 290 nm; **1a**, **1b**, **1g**, and **2b**: λ_{ex} = 320 nm) over 300−600 s. In each case, except for **5b**, the fluorescence intensity changed by less than 1% (see the Supporting Information for details). For this unsubstituted purine, even in thoroughly degassed CH_2Cl_2, the peak intensity decreased ∼5% during each of three consecutive 5-min exposures. The decomposition of the compound was confirmed by TLC and ^{1}H NMR, although the mixture was too complex to interpret. Worth noting, the absorption spectra of both the original compound and the decomposition mixture are similar and the mixture maintains its fluorescence (although λ_{em} is red-shifted to 377 nm); in other words, simply monitoring the absorbance does not reliably report on the integrity of the sample. In the remaining three solvents, all tested compounds, except for **5b** and **1b**, are photochemically stable. The former shows decomposition in all three, while **1b** is sensitive in 1,4-dioxane and methanol (ester **2b** is stable in these solvents).

Electronic Structure Calculations. Both semiempirical and high-level DFT calculations have been used to shed light on the electronic structure of the donor−acceptor purines. The ground-state geometries, dipoles, and orbital energies have been obtained from DFT calculations at the B3LYP/6-311++G** level (as implemented in Gaussian 03[63]). In all cases benzyl groups (Bn) have been abbreviated as methyl substituents (Me) to reduce computational cost (the truncated compounds are referred to as **1b-Me**, **2c-Me**, etc.), and frequency calculations have been performed to assign the optimized geometries as energy minima or transition states. For esters **2-Me** and the amide **3 g-Me**, the initial acceptor geometries used were the ones identified by X-ray crystallography (Figure 2). To demonstrate the accuracy of the calculations, Table S2 compares the bond lengths for 2-AP[14c] and **1e** from their X-ray crystal

(57) (a) Ravi, M.; Soujanya, T.; Samanta, A.; Radhakrishnan, T. P. *J. Chem. Soc., Faraday Trans.* **1995**, *91*, 2739–2742. (b) Ravi, M.; Samanta, A.; Radhakrishnan, T. P. *J. Phys. Chem.* **1994**, *98*, 9133–9136.
(58) (a) Wong, M. W.; Wiberg, K. B.; Frisch, M. J. *J. Comput. Chem.* **1995**, *16*, 385–394. (b) Karelson, M. M.; Zerner, M. C. *J. Phys. Chem.* **1992**, *96*, 6949–6957. (c) Wong, M. W.; Frisch, M. J.; Wiberg, K. B. *J. Am. Chem. Soc.* **1991**, *113*, 4776–4782. (d) Edward, J. T. *J. Chem. Educ.* **1970**, *47*, 261–270.
(59) Available free from http://accelrys.com.
(60) Similar values (within 0.1 Å) come from an alternative equation that does not scale the calculated volume by 1.33, but rather adds 0.5 Å to the final value of *a*.
(61) (a) Broo, A.; Holmén, A. *Chem. Phys.* **1996**, *211*, 147–161. (b) Gryczyński, I.; Kawski, A. *Bull. Acad. Pol. Sci., Ser. Sci., Math., Astron. Phys.* **1977**, *25*, 1189–1196.
(62) (a) Rachofsky, E. L.; Osman, R.; Ross, J. B. A. *Biochemistry* **2001**, *40*, 946–956. (b) Kawski, A.; Bartoszewicz, B.; Gryczyński, I.; Krajewski, M. *Bull. Acad. Pol. Sci., Ser. Sci., Math., Astron. Phys.* **1975**, *23*, 367–372.
(63) Frisch, M. J. T., et al. Gaussian, Inc.: Wallingford, CT, 2004.

Table 8. Electronic Structure Data for **5a-Me** and **1**−**3-Me**[a]

purine	μ_g	HOMO calcd (eV)	LUMO calcd (eV)	ΔE calcd (eV)	ΔE optical (eV) [λ_{cutoff} (nm)][b]
5a-Me	3.85	−6.03	−1.23	4.80	3.7 [332]
1a-Me	5.45	−6.52	−2.27	4.25	3.5 [352]
1b-Me	5.96	−6.24	−2.21	4.03	3.2 [385]
1c-Me	6.13	−6.08	−2.14	3.94	3.0 [410]
1d-Me	6.60	−6.29	−1.87	4.42	3.5 [352]
1e-Me	5.00	−5.88	−1.68	4.20	3.4 [368]
1f-Me[c]	5.66	−5.75	−1.68	4.07	3.1 [396]
1 g-Me	5.52	−5.64	−1.60	4.04	3.2 [385]
2a-Me	5.19	−6.24	−2.04	4.20	3.4 [370]
2b-Me	5.31	−5.97	−1.99	3.98	3.2 [385]
2c-Me	5.42	−5.82	−1.94	3.88	3.0 [410]
2d-Me	4.74	−6.03	−1.69	4.34	3.5 [355]
2e-Me	2.43	−5.62	−1.55	4.07	3.3 [380]
2f-Me	3.16	−5.53	−1.56	3.97	3.2 [390]
2 g-Me	2.81	−5.40	−1.48	3.92	3.1 [405]
3 g-Me[d]	3.36	−5.36	−1.25	4.11	3.2 [386]

[a] See the Supporting Information for computational details. All benzyl groups have been replaced by methyl groups for the calculations. [b] Determined for **1**−**3** based on UV absorption data in CH_2Cl_2. The λ_{cutoff} is defined here as the wavelength after the lowest energy λ_{max} where there is less than a 200 M^{-1} cm^{-1} variation over a 5 nm range (procedure according to ref 19a). [c] One imaginary frequency was identified for this structure indicating a transition state. The frequency is associated with minor inversion of the C(2) amino group based on analysis of the structure coordinate file. [d] Acceptor = $CONHCH_3$.

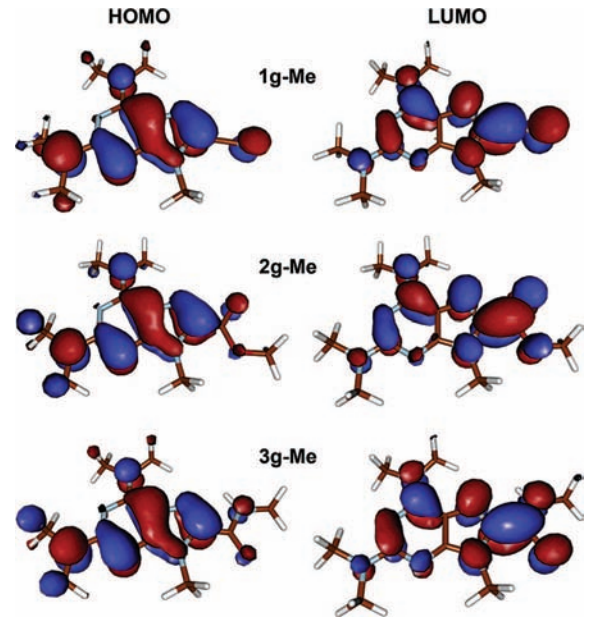

Figure 7. Representative orbital density plots (Molden v. 4.6) for the D−A purines calculated from B3LYP/6-31++G** optimized geometries. The HOMO (left) and LUMO (right) levels for series **g-Me** are shown (Table 7).

structures with the calculated 9-methyl analogues, **5a-Me** and **1e-Me**, respectively. The values are the same within ∼0.02 Å. Likewise, the calculated ground-state dipole moment for **5a-Me** (3.85 D at the B3LYP/6-31++G** level) is similar to the literature calculated value of 3.64 D (method = CASSCF (10,14 CAS)).[141] Nearly all of the optimized geometries do show a slight pyramidalization of the C(2) and C(6) amino (or dimethylamino) nitrogens (overall C_1 symmetry), consistent with the X-ray crystal structure of 2-AP[14c] and other calculated purine structures.[14a,f,m] The distortion has small energetic consequences;[14f,m] constraining the geometry of the dimethylamino group of **1e**, for example, provides no change in ground-state dipole moment or in the HOMO and LUMO energies.

Summarized in Table 8 are the dipole and orbital energy data obtained for **1**-**3-Me** from the DFT calculations. Complementary orbital density plots of the HOMO and LUMO levels could be generated using Molden v. 4.6[64] to show graphically the electronic nature of the ground states (Figure 7 shows the **g-Me** series; others can be found in the Supporting Information). The orbital features are quite similar within and between the nitriles, methyl esters, and amides. The HOMO consists of delocalized π orbitals on the purine plane, with the greatest density in the N(9)−C(4)−C(5)−C(6) region (see Figure 1 for atom labels) consistent with what has been observed for parent 2-AP.[14e,l] Localized p_z orbitals are seen on the exocyclic donor heteroatoms and the acceptor functionality, and there is slightly more charge separation in the HOMO for the nitriles (consistent also with their greater ground-state dipole moments; average for nitriles = 5.77 D, esters = 4.15 D). The LUMO is also of π character *but more concentrated on the acceptor substituent*, the cyano group, methyl ester, or amide. Generally the density on the C(2) donor group diminishes most substantially in the LUMO; the C(6) donor orbital coefficient is only slightly affected. The degree of charge separation in the molecules is modest, but consistent with the experimental $\Delta\mu_{ge}$ values (vide supra) and similarly structured fluorophores.

Some familiar trends emerge from Table 8. Comparing **a**−**c-Me**, the HOMO and LUMO energies and ground-state dipole moments (μ_g) increase with increasing donor strength at C(2), and **1c-Me** has the lowest calculated HOMO−LUMO gap. The computational data parallels the experimental results where **1c** (versus **1b** or **1a**) has the most red-shifted abs λ_{max} and lowest optical band gap. Comparison of **1a**−**c-Me** and **2a**−**c-Me** further shows that the esters (**2**) generally bring slightly lower HOMO−LUMO gaps *and* μ_g values in the gas-phase, differences that do not emerge in solution. There is overall good agreement between the *trends* in the calculated HOMO−LUMO gaps and the optical gaps calculated from the onset of the low-energy absorption maximum, although the former tend to be up to 0.9 eV larger. Preliminary cyclic voltammetry (CV) data collected for **1e**−**g** in CH_2Cl_2 suggests that the calculated HOMO values may be a bit low (0.2−0.4 eV) and the calculated LUMO values a bit high (0.5−0.9 eV).[65] Finally, ZINDO/S CI semiempirical calculations[66] (see the Supporting Information for details) using the optimized DFT ground-state geometries show that the lowest energy transition for the D−A purines is associated with promotion of an electron from the HOMO to the LUMO in all cases ($S_0 \rightarrow S_1$). Given the large CI coefficient for this transition (∼0.6), it is an allowed process for which the trend in energy gap (327−354 nm; 3.79−3.50 eV) correlates well with the trend in λ_{max} in CH_2Cl_2 (311−362 nm; 3.99−3.43 eV).

Conclusions

"Push−pull" purines have been prepared by the introduction of electron-accepting functional groups (−CN, $-CO_2CH_3$, −CONHR) to the heterocyclic C(8) position to complement typical electron-releasing groups at C(2) and C(6). The chemical

(64) Available from www.cmbi.ru.nl/molden/molden.html (see Schaftenaar, G. N., J. H. *J. Comput.-Aided Mol. Design* **2000**, *14*, 123−134).

(65) Data will be reported separately.

(66) Ridley, J. E.; Zerner, M. C. *Theor. Chim. Acta* **1976**, *42*, 223–236.

modifications result in significantly improved photophysical properties relative to the acceptor-free molecules, important with respect to potential biosensing or materials applications. These include (1) red-shifted (20−50 nm) absorption maxima; (2) highly solvatochromic emission profiles (em λ_{max} from 355−466 nm depending on substitution pattern and solvent); (3) significantly enhanced (up to 2500%) fluorescence quantum yields (providing among the highest values for purines known); and (4) improved photochemical stability upon continuous irradiation. Access to carboxamides **3** using conventional peptide-coupling chemistry demonstrates one approach to elaborating the fluorophores while maintaining, even enhancing, their optical properties. Derivatives like **3f** that bear primary amino groups further speak to use of the molecules as unnatural amino acids, where their interesting molecular recognition features and optical properties could be used in synthetic peptide architectures.

Comprehensive structure−property relationships for the purines have emerged from analysis of their photophysical data in various solvents. While the absorption and emission maxima have been shown to depend on donor and acceptor structure, relative donor position, and medium in understandable ways, the quantum yields have varied less intuitively. Ester (**b**) and amide (**c**) acceptor groups have served to partially "neutralize" the quantum yield sensitivity to solvent polarity that is otherwise observed within the nitriles **a** and many other donor-π-acceptor systems. Given this feature and that the acceptor-modified purines enjoy excellent linear correlations between emission energy and solvent polarity (E_T^N), the molecules should be useful in microenvironment sensing applications. Lastly, a quantitative treatment of the solvent-dependent emission data has provided insight into electronic structure; the calculated $\Delta\mu_{ge}$ values (2.1−3.4 D), for example, are consistent with the degree of charge separation reflected in calculated molecular orbital plots.

There is much left to do to exploit the "information content" of biology's heterocycles within niche materials and sensing applications, and this pursuit is likely to offer both fundamental and practical advances. Two avenues are available now that we have imparted useful photophysical properties to simple purines using readily modified substituents. Toward biological and sensing applications, we are currently developing water soluble versions of the purines that will allow us to understand how they perform in biomolecular microenvironments. Encouraging is that C(8) substituents like −CN, $-CO_2CH_3$, and $-CONHCH_3$ appear not much larger than the vinyl ($CH{=}CH_2$) group known to be tolerated by the DNA duplex.[67] On the materials side we are exploring applications wherein efficient small-molecule fluorophores have traditionally been successful, with the ultimate goal of drawing (biorelevant)structure−function relationships in this context. Useful in both cases will be purines that mirror the better of the donor−acceptor arrangements presented here *and* preserve at least one hydrogen-bonding edge for molecular recognition. 2,6-Diaminopurine derivatives are promising targets in this regard given that they are compatible with DNA, RNA, and PNA structure and complementary to uracil and thymine.[68]

Acknowledgement. We are grateful to the University of Florida, the Donors of the American Chemical Society Petroleum Research Fund (PRF Grant No. 42229-G4), and the Research Corporation (Research Innovation Award to R.K.C.) for financial support. R.S.B. is a University of Florida Alumni Graduate Fellow. We thank Priya Vijapura, funded through the UF Student Science Training Program, Andrea K. Myers, funded through the NSF REU program (CHE-0139505), and Prabhu Bellarmine for help with initial spectroscopic studies. We additionally thank Aubrey L. Dyer for preliminary CV measurements and Dr. Bobby V. Sumpter (Center for Nanophase Materials Sciences, Oak Ridge National Laboratory) for computational advice. K.A.A. thanks the National Science Foundation and University of Florida for funding the X-ray crystallography equipment. We especially thank Dr. Katsu Ogawa, Prof. Adrian Roitberg, Prof. Kirk Schanze, and Prof. Linda Bloom for guidance and/or instrument access.

Supporting Information Available: Experimental procedures and characterization data, crystallographic data for **2f** and **3f**, additional photophysical data (including representative photostability studies), computational details (including additional molecular orbital plots and Cartesian coordinates and energies for geometry-optimized structures), copies of ^{1}H NMR spectra for all new compounds, and complete ref 63. This material is available free of charge via the Internet at http://pubs.acs.org.

JA806348Z

(67) Gaied, N. B.; Glasser, N.; Ramalanjaona, N.; Beltz, H.; Wolff, P.; Marquet, R.; Burger, A.; Mély, Y. *Nucleic Acids Res.* **2005**, *33*, 1031–1039.

(68) (a) Pasternak, A.; Kierzek, E.; Pasternak, K.; Turner, D. H.; Kierzek, R. *Nucleic Acids Res.* **2007**, *35*, 4055–4063. (b) Haaima, G.; Hansen, H. F.; Christensen, L.; Dahl, O.; Nielsen, P. E. *Nucleic Acids Res.* **1997**, *25*, 4639–4643. (c) Gaffney, B. L.; Marky, L. A.; Jones, R. A. *Tetrahedron* **1984**, *40*, 3–13.